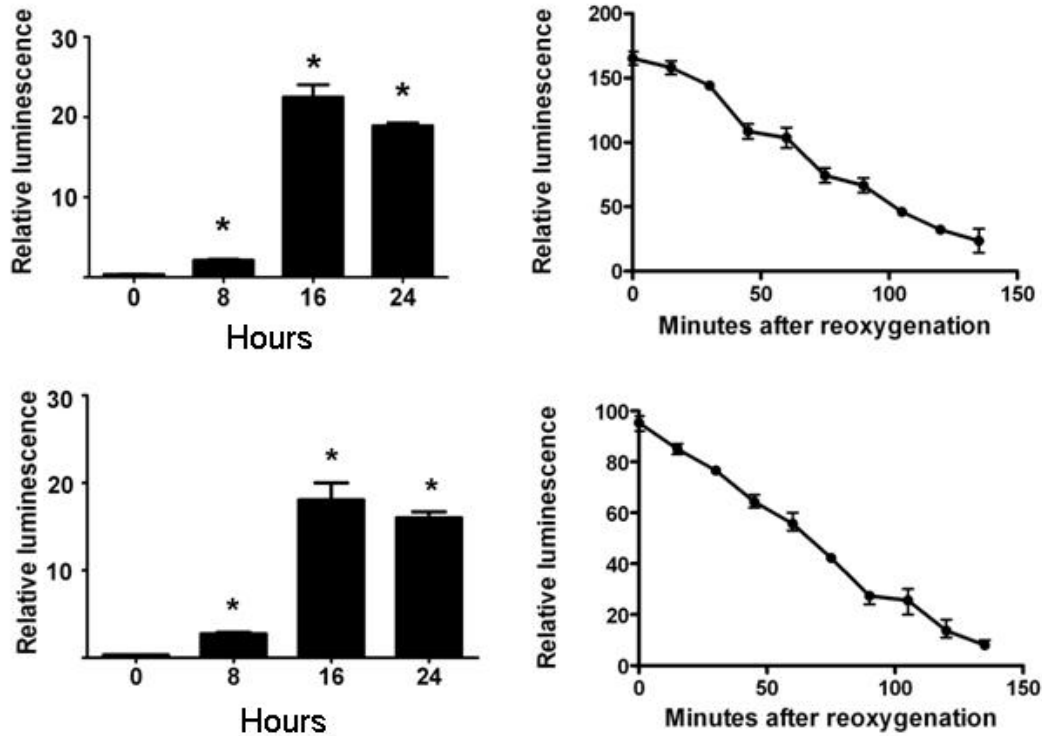
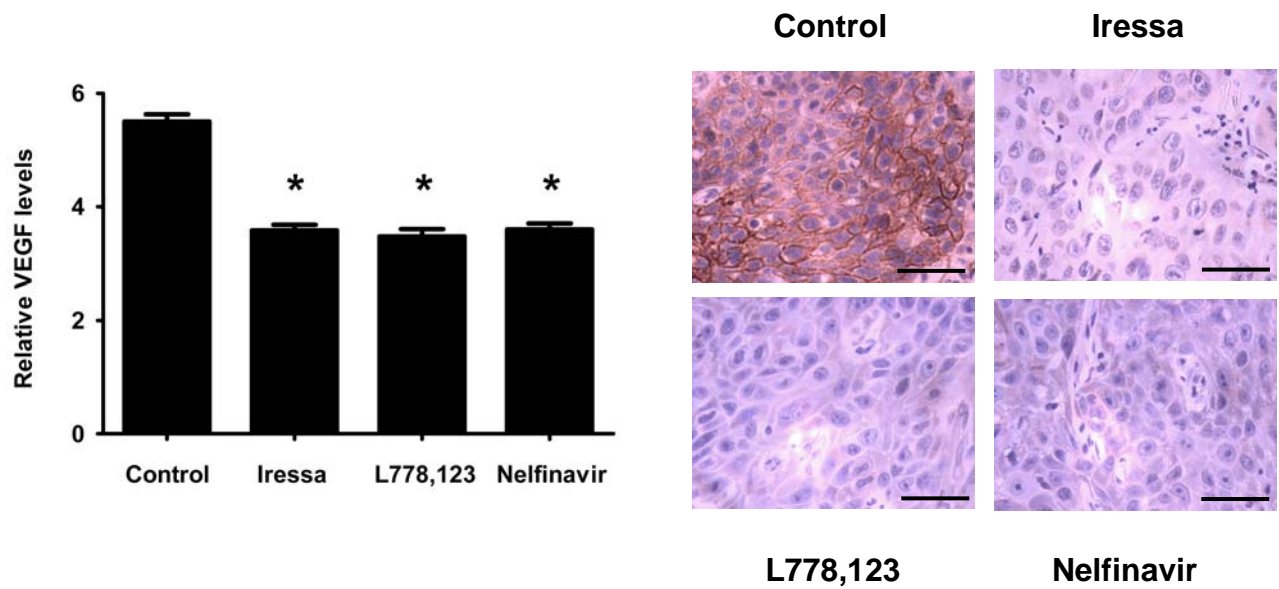


Qayum et al. Supplementary Figures.



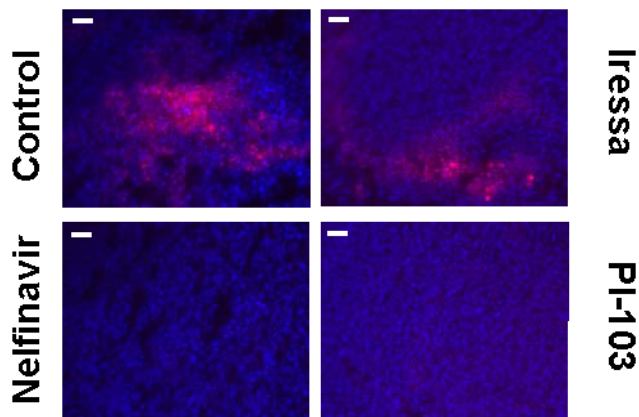
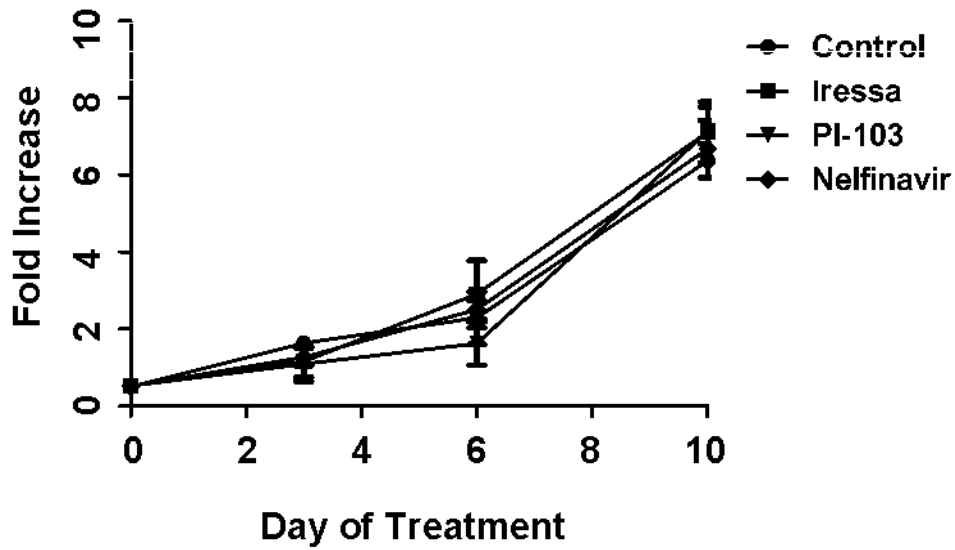
Supplementary Figure 1: Induction of luciferase expression under hypoxia.

HT1080 (top, left) and SQ20B (bottom, left) cell lines stably transfected with HRE-luciferase constructs were tested under for luciferase expression (Steady-glo, Promega) under hypoxia (0.1% O₂) for 8, 16 and 24h. Right panels: Quantification of luminescence signal in live cells after reoxygenation in air in HT1080 (top, right) and SQ20B (bottom, right). Data calculated from IVIS images of luciferin luminescence.



Supplementary Figure 2: VEGF levels and CA-9 expression in SQ20B tumors are both reduced after signaling inhibition.

VEGF Levels determined by ELISA (left), are relative to positive controls provided in with the assay (VEGF Quantikine, R&D systems). CA-9 expression by immunohistochemical staining (right) (Scale bar denotes 100 μ m).

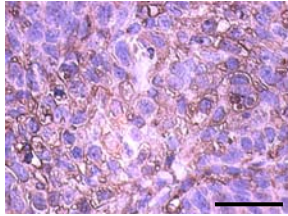


Supplementary Figure 3: HT1080 Tumor growth and EF5 binding

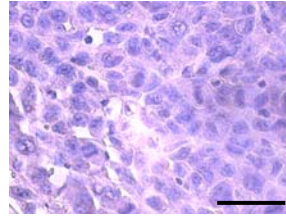
Top: HT1080 xenograft tumor growth measured throughout the time of inhibitor treatment is unaffected by signaling inhibition ($p=0.9987$, ANOVA)

Bottom: Immunohistochemistry confirms a reduction in EF5 binding in HT1080 tumors treated with PI-103 and Nelfinavir but not Iressa.

SQ20B

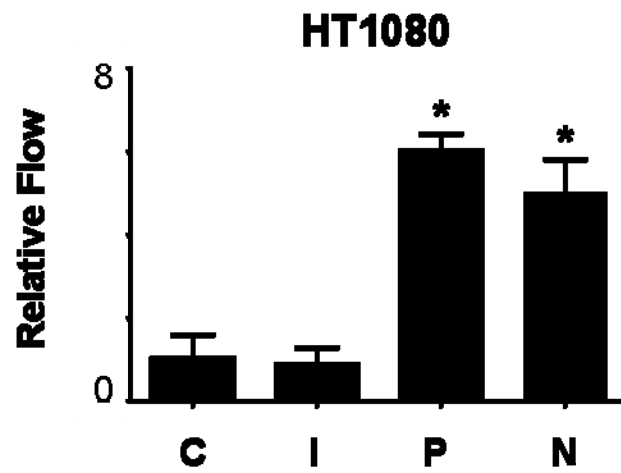


HT1080



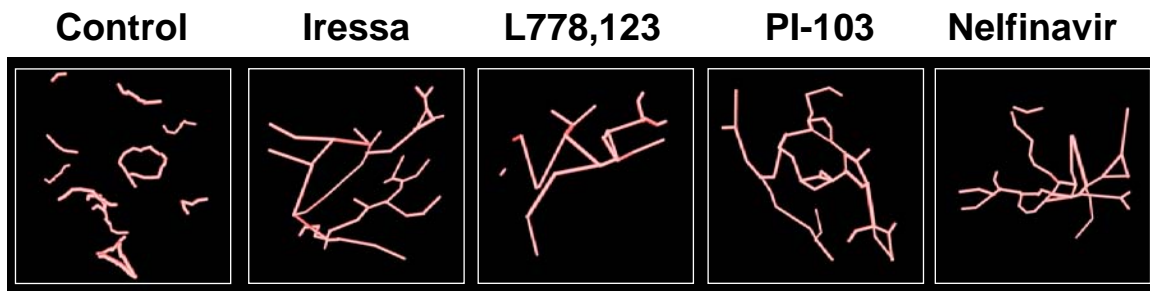
Supplementary Figure 4: Immunohistochemical staining for EGFR.

Expression of EGFR is seen in SQ20B xenografts while HT1080 xenografts lack detectable EGFR. (Scale bar denotes 100 μ m)



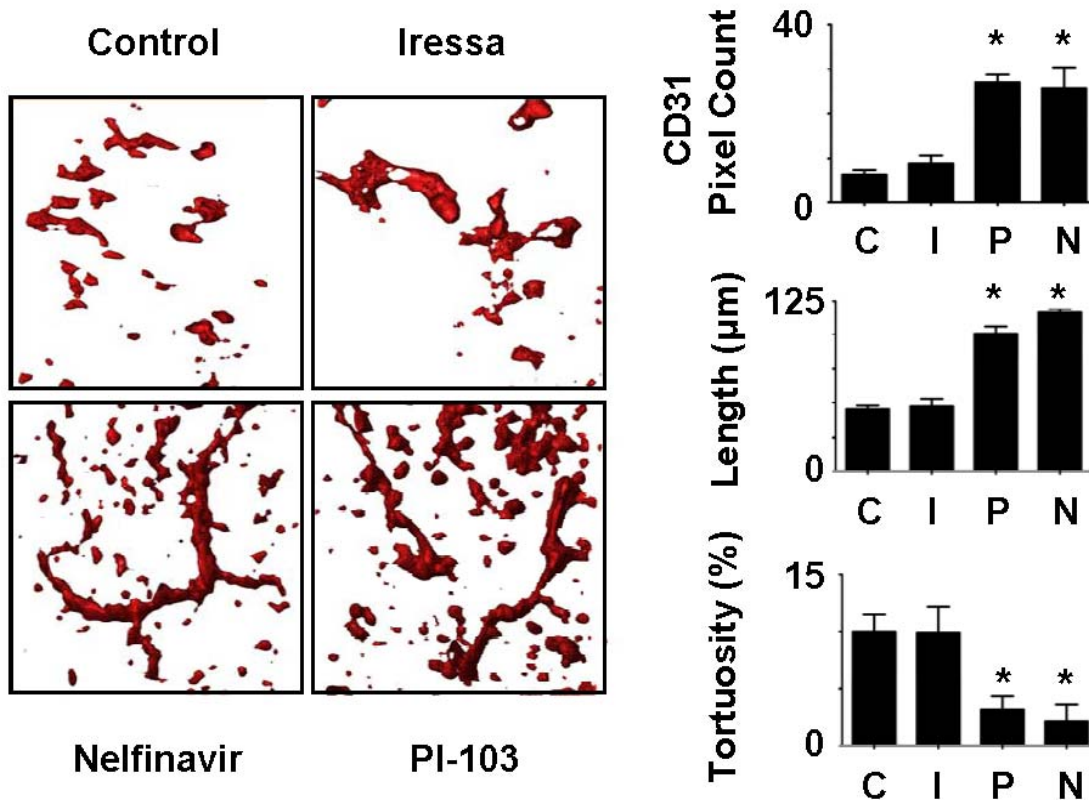
Supplementary Figure 5: Tumor blood flow in HT1080 xenografts.

Blood flow changes are seen in HT1080 tumour xenografts treated with Nelfinavir (N) and PI-103 (P), as compared to controls (C). This change is not seen with Iressa (I). All values are relative to controls (=1).



Supplementary Figure 6: Changes in 3D vascular structure after signaling inhibition.

Representative computer generated tracings of vasculature from 3D reconstructions of SQ20B tumors using Trace3D software. These were used to calculate internodal vessel length and tortuosity.

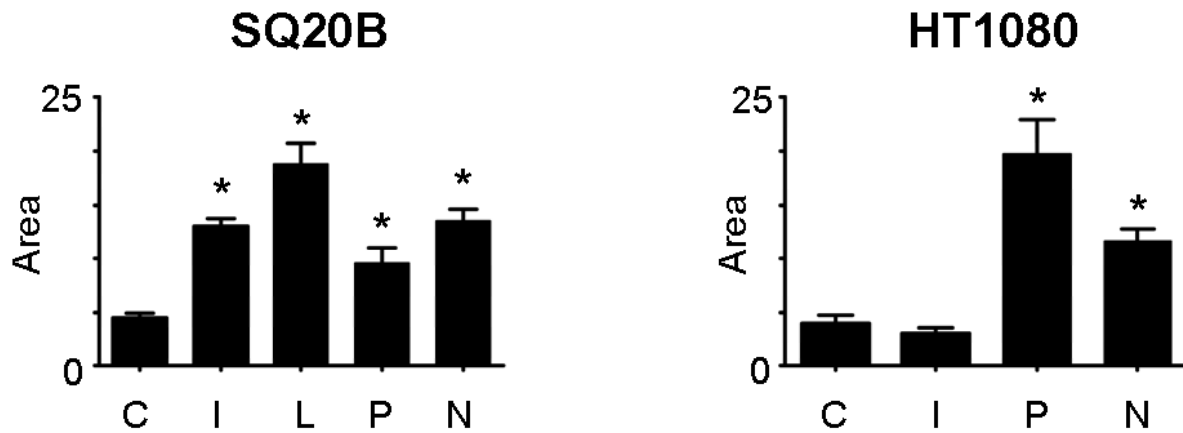
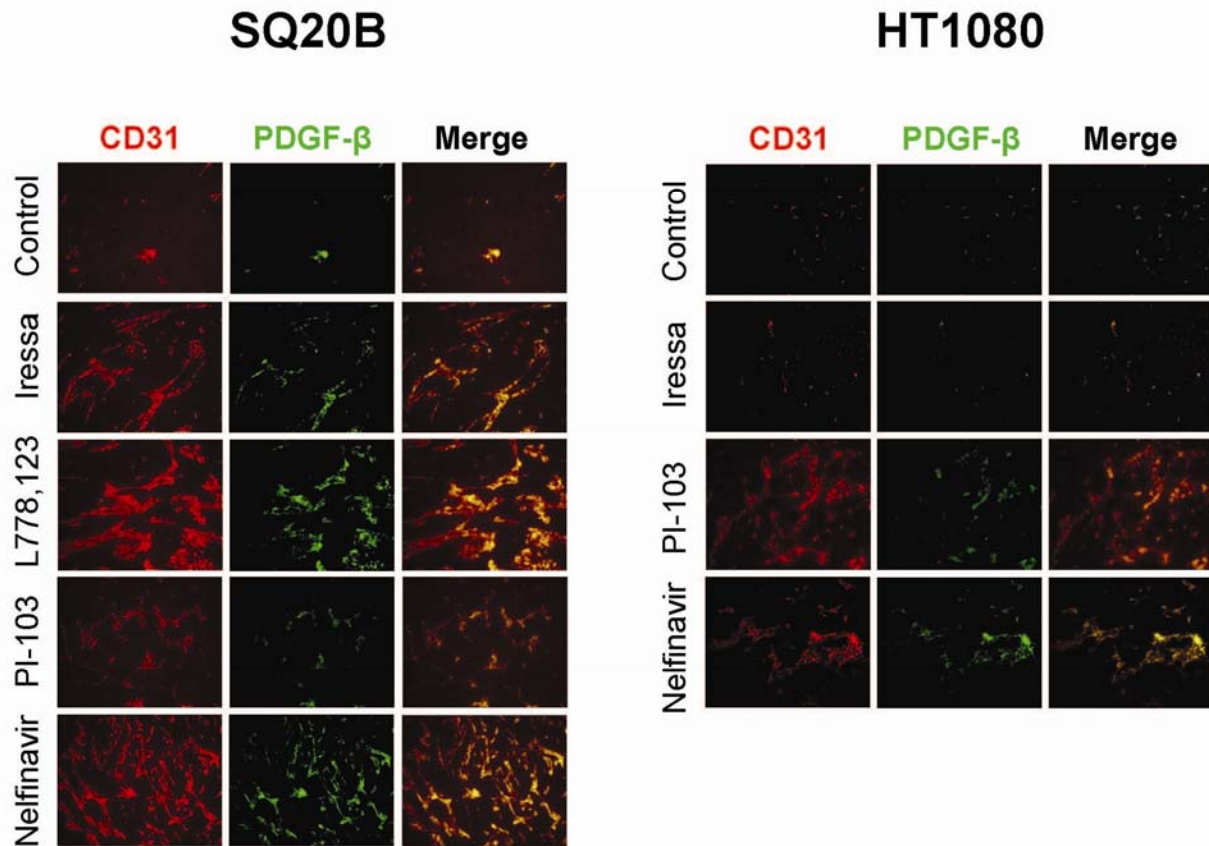


Supplementary Figure 7: HT1080 tumor xenografts demonstrate normalized vascular morphology.

Xenograft tumors in SCID mice were generated from the HT1080 cell line. Mice bearing tumors were treated with Iressa (I), PI-103 (P) or Nelfinavir (N) for 10 days. CD31-PE was injected at 10 minutes respectively prior to sacrifice. * indicates $p < 0.05$ using two tailed t-tests compared to controls.

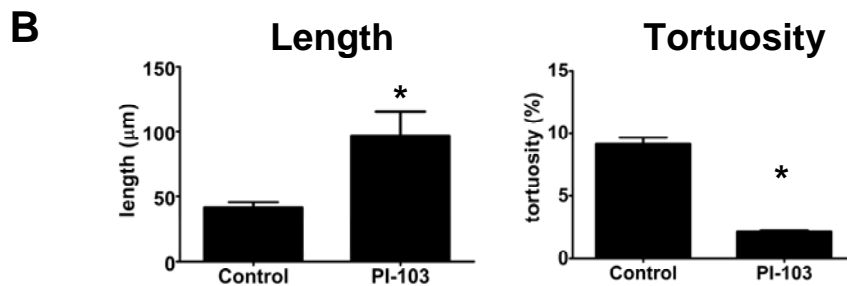
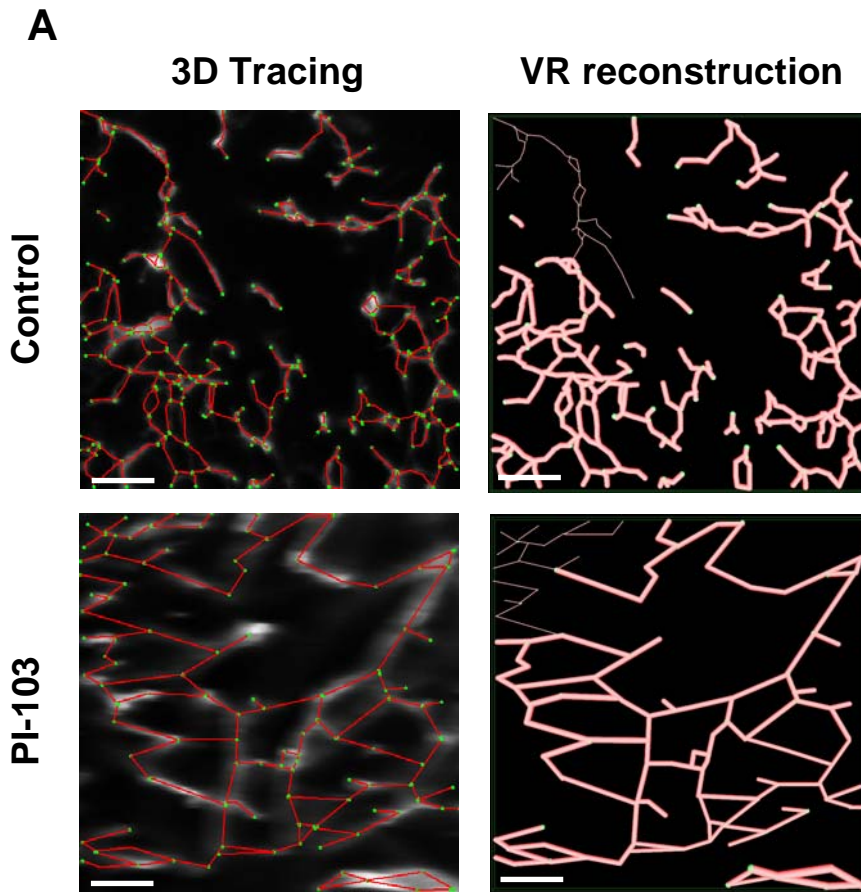
Left: 100µm 3D reconstructions of vascular morphology (red) demonstrating vascular normalization after signaling inhibition using Nelfinavir and PI-103, but not Iressa (20X magnification)

Right: Quantitation of perfused vessel density, uninterrupted vessel length and tortuosity.



Supplementary Figure 8: Changes in vessel maturity in treated tumor xenografts .

Evaluation and quantitation of vessel maturity by immunohistochemical staining for PDGF- β in SQ20B xenografts (Left) and HT1080 xenografts (right). * indicates $p < 0.05$. Images were taken using 20X magnification. Increased PDGF- β was observed after all treatments except Iressa in the HT1080 xenograft model.



Supplementary Figure 9: Changes in MMTV-Neu vascular morphology after PI3 kinase inhibition.

(A) Examples of Trace3D software tracings (left) and virtual reality reconstructions (right) from MMTV-Neu control tumors and after treatment with PI-103.

(B) Quantitative analysis reveals increased average length between nodes and decreased percentage tortuosity.